Search for a Light Sterile Neutrino at Daya Bay

F. P. An,[1] A. B. Balantekin,[2] H. R. Band,[2] W. Beriguete,[3] M. Bishai,[3] S. Blyth,[4] I. Butorov,[5] G. F. Cao,[6] J. Cao,[6] Y.L. Chan,[7] J. F. Chang,[6] L. C. Chang,[8] Y. Chang,[9] C. Chasman,[3] H. Chen,[6] Q. Y. Chen,[10] S. M. Chen,[11] X. Chen,[7] X. Chen,[6] Y. X. Chen,[12] Y. Chen,[13] Y. P. Cheng,[6] J. J. Cherwinka,[2] M. C. Chu,[7] J. P. Cummings,[14] J. de Arcos,[15] Z. Y. Deng,[6] Y. Y. Ding,[6] M. V. Diwan,[3] E. Draeger,[15] X. F. Du,[6] D. A. Dwyer,[16] W. R. Edwards,[16] S. R. Ely,[17] J. Y. Fu,[6] L. Q. Ge,[18] R. Gill,[3] M. Gonchar,[5] G. H. Gong,[11] H. Gong,[11] M. Grassi,[6] W. Q. Gu,[19] M. Y. Guan,[6] X. H. Guo,[20] R. W. Hackenburg,[3] G. H. Han,[21] S. Hans,[3] M. He,[6] K. M. Heeger,[2,22] Y. K. Heng,[6] P. Hinrichs,[2] Y. K. Hor,[23] Y. B. Hsiung,[4] B. Z. Hu,[8] L. M. Hu,[3] L. J. Hu,[20] T. Hu,[6] W. Hu,[6] E. C. Huang,[17] H. Huang,[24] X. T. Huang,[10] P. Huber,[23] G. Hussain,[11] Z. Isvan,[3] D. E. Jaffe,[3] P. Jaffke,[23] K. L. Jen,[8] S. Jetter,[6] X. P. Ji,[25] X. L. Ji,[6] H. J. Jiang,[18] J. B. Jiao,[10] R. A. Johnson,[26] L. Kang,[27] S. H. Kettell,[3] M. Kramer,[16,28] K. K. Kwan,[7] M.W. Kwok,[7] T. Kwok,[29] W. C. Lai,[18] K. Lau,[30] L. Lebanowski,[11] J. Lee,[16] R. T. Lei,[27] R. Leitner,[31] A. Leung,[29] J. K. C. Leung,[29] C. A. Lewis,[2] D. J. Li,[32] F. Li,[18,6] G. S. Li,[19] Q. J. Li,[6] W. D. Li,[6] X. N. Li,[6] X. Q. Li,[25] Y. F. Li,[6] Z. B. Li,[33] H. Liang,[32] C. J. Lin,[16] G. L. Lin,[8] P.Y. Lin,[8] S. K. Lin,[30] Y. C. Lin,[18] J. J. Ling,[3,17] J. M. Link,[23] L. Littenberg,[3] B. R. Littlejohn,[26] D. W. Liu,[30] H. Liu,[30] J. L. Liu,[19] J. C. Liu,[6] S. S. Liu,[29] Y. B. Liu,[6] C. Lu,[34] H. Q. Lu,[6] K. B. Luk,[28,16] Q. M. Ma,[6] X. Y. Ma,[6] X. B. Ma,[12] Y. Q. Ma,[6] K. T. McDonald,[34] M. C. McFarlane,[2] R.D. McKeown,[35,21] Y. Meng,[23] I. Mitchell,[30] J. Monari Kebwaro,[36] Y. Nakajima,[16] J. Napolitano,[37] D. Naumov,[5] E. Naumova,[5] I. Nemchenok,[5] H. Y. Ngai,[29] Z. Ning,[6] J. P. Ochoa-Ricoux,[38,16] A. Olshevski,[5] S. Patton,[16] V. Pec,[31] J. C. Peng,[17] L. E. Piilonen,[23] L. Pinsky,[30] C. S. J. Pun,[29] F. Z. Qi,[6] M. Qi,[39] X. Qian,[3] N. Raper,[40] B. Ren,[27] J. Ren,[24] R. Rosero,[3] B. Roskovec,[31] X. C. Ruan,[24] B. B. Shao,[11] H. Steiner,[28,16] G. X. Sun,[6] J. L. Sun,[41] Y. H. Tam,[7] X. Tang,[6] H. Themann,[3] K. V. Tsang,[16] R. H. M. Tsang,[35] C.E. Tull,[16] Y. C. Tung,[4] B. Viren,[3] V. Vorobel,[31] C. H. Wang,[9] L. S. Wang,[6] L. Y. Wang,[6] M. Wang,[10] N. Y. Wang,[20] R. G. Wang,[6] W. Wang,[21,33] W. W. Wang,[39] X. Wang,[42] Y. F. Wang,[6] Z. Wang,[11] Z. Wang,[6] Z. M. Wang,[6] D. M. Webber,[2] H. Y. Wei,[11] Y. D. Wei,[27] L. J. Wen,[6] K. Whisnant,[43] C. G. White,[15] L. Whitehead,[30] T. Wise,[2] H. L. H. Wong,[28,16] S. C. F. Wong,[7] E. Worcester,[3] Q. Wu,[10] D. M. Xia,[6] J. K. Xia,[6] X. Xia,[10] Z. Z. Xing,[6] J. Y. Xu,[7] J. L. Xu,[6] J. Xu,[20] Y. Xu,[25] T. Xue,[11] J. Yan,[36] C. C. Yang,[6] L. Yang,[27] M. S. Yang,[6] M. T. Yang,[10] M. Ye,[6] M. Yeh,[3] Y. S. Yeh,[8] B. L. Young,[43] G. Y. Yu,[39] J. Y. Yu,[11] Z. Y. Yu,[6] S. L. Zang,[39] B. Zeng,[18] L. Zhan,[6] C. Zhang,[3] F. H. Zhang,[6] J. W. Zhang,[6] Q. M. Zhang,[36] Q. Zhang,[18] S. H. Zhang,[6] Y. C. Zhang,[32] Y. M. Zhang,[11] Y. H. Zhang,[6] Y. X. Zhang,[41] Z. J. Zhang,[27] Z. Y. Zhang,[6] Z. P. Zhang,[32] J. Zhao,[6] Q. W. Zhao,[6] Y. Zhao,[12,21] Y. B. Zhao,[6] L. Zheng,[32] W. L. Zhong,[6] L. Zhou,[6] Z. Y. Zhou,[24] H. L. Zhuang,[6] and J. H. Zou[6]

(The Daya Bay Collaboration)

[1]*Institute of Modern Physics, East China University of Science and Technology, Shanghai*
[2]*University of Wisconsin, Madison, Wisconsin, USA*
[3]*Brookhaven National Laboratory, Upton, New York, USA*
[4]*Department of Physics, National Taiwan University, Taipei*
[5]*Joint Institute for Nuclear Research, Dubna, Moscow Region*
[6]*Institute of High Energy Physics, Beijing*
[7]*Chinese University of Hong Kong, Hong Kong*
[8]*Institute of Physics, National Chiao-Tung University, Hsinchu*
[9]*National United University, Miao-Li*
[10]*Shandong University, Jinan*
[11]*Department of Engineering Physics, Tsinghua University, Beijing*
[12]*North China Electric Power University, Beijing*
[13]*Shenzhen University, Shenzhen*
[14]*Siena College, Loudonville, New York, USA*
[15]*Department of Physics, Illinois Institute of Technology, Chicago, Illinois, USA*
[16]*Lawrence Berkeley National Laboratory, Berkeley, California, USA*
[17]*Department of Physics, University of Illinois at Urbana-Champaign, Urbana, Illinois, USA*
[18]*Chengdu University of Technology, Chengdu*
[19]*Shanghai Jiao Tong University, Shanghai*
[20]*Beijing Normal University, Beijing*
[21]*College of William and Mary, Williamsburg, Virginia, USA*
[22]*Department of Physics, Yale University, New Haven, Connecticut, USA*
[23]*Center for Neutrino Physics, Virginia Tech, Blacksburg, Virginia, USA*
[24]*China Institute of Atomic Energy, Beijing*
[25]*School of Physics, Nankai University, Tianjin*
[26]*Department of Physics, University of Cincinnati, Cincinnati, Ohio, USA*
[27]*Dongguan University of Technology, Dongguan*
[28]*Department of Physics, University of California, Berkeley, California, USA*
[29]*Department of Physics, The University of Hong Kong, Pokfulam, Hong Kong*

[30]*Department of Physics, University of Houston, Houston, Texas, USA*
[31]*Charles University, Faculty of Mathematics and Physics, Prague*
[32]*University of Science and Technology of China, Hefei*
[33]*Sun Yat-Sen (Zhongshan) University, Guangzhou*
[34]*Joseph Henry Laboratories, Princeton University, Princeton, New Jersey, USA*
[35]*California Institute of Technology, Pasadena, California, USA*
[36]*Xi'an Jiaotong University, Xi'an*
[37]*Department of Physics, College of Science and Technology, Temple University, Philadelphia, Pennsylvania, USA*
[38]*Institute of Physics, Pontifical Catholic University of Chile, Santiago, Chile*
[39]*Nanjing University, Nanjing*
[40]*Department of Physics, Applied Physics, and Astronomy, Rensselaer Polytechnic Institute, Troy, New York, USA*
[41]*China General Nuclear Power Group*
[42]*College of Electronic Science and Engineering, National University of Defense Technology, Changsha*
[43]*Iowa State University, Ames, Iowa, USA*
(Dated: October 10, 2014)

A search for light sterile neutrino mixing was performed with the first 217 days of data from the Daya Bay Reactor Antineutrino Experiment. The experiment's unique configuration of multiple baselines from six 2.9 $\mathrm{GW_{th}}$ nuclear reactors to six antineutrino detectors deployed in two near (effective baselines 512 m and 561 m) and one far (1579 m) underground experimental halls makes it possible to test for oscillations to a fourth (sterile) neutrino in the $10^{-3}\ \mathrm{eV}^2 < |\Delta m^2_{41}| < 0.3\ \mathrm{eV}^2$ range. The relative spectral distortion due to electron antineutrino disappearance was found to be consistent with that of the three-flavor oscillation model. The derived limits on $\sin^2 2\theta_{14}$ cover the $10^{-3}\ \mathrm{eV}^2 \lesssim |\Delta m^2_{41}| \lesssim 0.1\ \mathrm{eV}^2$ region, which was largely unexplored.

PACS numbers: 14.60.Pq, 14.60.St, 29.40.Mc, 28.50.Hw, 13.15.+g
Keywords: sterile neutrino, neutrino mixing, reactor neutrino, Daya Bay

Measurements in the past decades have revealed large mixing between the flavor and mass eigenstates of neutrinos. The neutrino mixing framework [1–3] with three flavors has been successful in explaining most experimental results, and several-percent precision has been attained in the determination of the neutrino mixing angles and the mass splittings. Despite this great progress, there is still room for other generations of neutrinos to exist. Fits to precision electroweak measurements [4, 5] have limited the number of light active neutrino flavors to three, although other light neutrinos may exist as long as they do not participate in standard V-A interactions. These neutrinos, which arise in extensions of the Standard Model that incorporate neutrino masses, are typically referred to as sterile neutrinos [2].

In addition to being well-motivated from the theoretical standpoint, sterile neutrinos are among the leading candidates to resolve outstanding puzzles in astronomy and cosmology. Sterile neutrinos with ∼keV masses are good candidates for non-baryonic Dark Matter [6, 7]. Light sterile neutrinos with eV or sub-eV mass have been shown to help reconcile the tensions in the cosmological data between current measurements of the present and early Universe [8] as well as between CMB and lensing measurements [9]. The recent B-mode polarization data from BICEP2 [10] has spurred even more discussion in this area [11–14].

If light sterile neutrinos mix with the three active neutrinos, their presence could be detected via the modification to the latter's oscillatory behavior. Various searches for active-sterile neutrino mixing in the mass-squared splitting $|\Delta m^2| > 0.1\ \mathrm{eV}^2$ region have been carried out in this way. The LSND [15] and MiniBooNE [16, 17] experiments observed excesses of electron (anti-)neutrino events in the muon (anti-)neutrino beams, which could be interpreted as sterile neutrino oscillation with $|\Delta m^2| \sim 1\ \mathrm{eV}^2$. However, these results are in tension [18–21] with the limits derived from other appearance [22–25] or disappearance searches [26–36]. Moreover, a reanalysis of the measured *vs.* predicted electron antineutrino events from previous reactor experiments has revealed a deficit of about 6% [37, 38]. Although the significance of this effect is still under discussion [39, 40], it is compatible with the so-called Gallium Anomaly [41–43] in that both can be explained by introducing a sterile neutrino with $|\Delta m^2| > 0.5\ \mathrm{eV}^2$ [44]. Until now however, the $|\Delta m^2| < 0.1\ \mathrm{eV}^2$ region has remained largely unexplored.

This Letter describes a search for a light sterile neutrino via its mixing with the active neutrinos using more than 300,000 reactor antineutrino interactions collected in the Daya Bay Reactor Antineutrino Experiment. This data set was recorded during the six-detector data period from December 2011 to July 2012. Since the antineutrino detectors are located at baselines ranging from a few hundred to almost two thousand meters away from the reactor cores, Daya Bay is most sensitive to active-sterile neutrino mixing in the $10^{-3}\ \mathrm{eV}^2 < |\Delta m^2| < 0.3\ \mathrm{eV}^2$ range. In this region, a positive signal for active-sterile neutrino mixing would predominantly manifest itself as an additional spectral distortion with a frequency different from the one due to the atmospheric mass splitting.

This work used a minimal extension of the Standard Model: the 3 (active) + 1 (sterile) neutrino mixing model. In this model, if the neutrino mass is much smaller than its momentum, the probability that an $\overline{\nu}_e$ produced with energy E is de-

tected as an $\overline{\nu}_e$ after traveling a distance L is given by

$$P_{\overline{\nu}_e \to \overline{\nu}_e} = 1 - 4 \sum_{i=1}^{3} \sum_{j>i}^{4} |U_{ei}|^2 |U_{ej}|^2 \sin^2 \Delta_{ji}. \quad (1)$$

Here U_{ei} is the element of the neutrino mixing matrix for the flavor eigenstate ν_e and the mass eigenstate ν_i, $\Delta_{ji} = 1.267 \Delta m^2_{ji}(\mathrm{eV}^2) \frac{L(\mathrm{m})}{E(\mathrm{MeV})}$ with $\Delta m^2_{ji} = m^2_j - m^2_i$ being the mass-squared difference between the mass eigenstates ν_j and ν_i. Using the parameterization of Ref. [34], U_{ei} can be expressed in terms of the neutrino mixing angles θ_{14}, θ_{13} and θ_{12}:

$$\begin{aligned} U_{e1} &= \cos\theta_{14} \cos\theta_{13} \cos\theta_{12}, \\ U_{e2} &= \cos\theta_{14} \cos\theta_{13} \sin\theta_{12}, \\ U_{e3} &= \cos\theta_{14} \sin\theta_{13}, \\ U_{e4} &= \sin\theta_{14}. \end{aligned} \quad (2)$$

If $\theta_{14} = 0$, the probability returns to the expression for three-neutrino oscillation.

The Daya Bay experiment has two near underground experimental halls (EH1 and EH2) and one far hall (EH3). Each hall houses functionally identical, three-zone antineutrino detectors (ADs) submerged in pools of ultra-pure water segmented into two optically decoupled regions. The water pools are instrumented with photomultiplier tubes (PMTs) to tag cosmic-ray-induced interactions. Reactor antineutrinos were detected via the inverse β-decay (IBD) reaction ($\overline{\nu}_e + p \to e^+ + n$). The coincidence of the prompt (e^+ ionization and annihilation) and delayed (n capture on Gd) signals efficiently suppressed the backgrounds, which amounted to less than 2% (5%) of the entire candidate samples in the near (far) halls [45]. The prompt signal measured the $\overline{\nu}_e$ energy with an energy resolution $\sigma_E/E \approx 8\%$ at 1 MeV. More details on the reconstruction and detector performance can be found in Ref. [46]. A summary of the IBD candidates used in this analysis, together with the baselines of the three experimental halls to each pair of reactors, is shown in Table I.

TABLE I. Total number of IBD candidates and baselines of the three experimental halls to the reactor pairs.

Location	IBD candidates	Mean Distance to Reactor Core (m)		
		Daya Bay	Ling Ao	Ling Ao-II
EH1	203809	365	860	1310
EH2	92912	1345	479	528
EH3	41589	1908	1536	1541

The uncertainty in the absolute energy scale of positrons was estimated to be about 1.5% through a combination of the uncertainties of calibration data and various energy models [45]. This quantity had a negligible effect on the sensitivity of the sterile neutrino search due to the relative nature of the measurement with functionally identical detectors. The uncertainty of the relative energy scale was determined from the relative response of all ADs to various calibration sources that spanned the IBD positron energy range, and was found to be 0.35%. The predicted $\overline{\nu}_e$ flux took into account the daily livetime-corrected thermal power, the fission fractions of each isotope as provided by the reactor company, the fission energies, and the number of antineutrinos produced per fission per isotope [47].

The precision of the measured baselines was about 2 cm with both the GPS and Total Station [48]. The geometric effect due to the finite size of the reactor cores and the antineutrino detectors, whose dimensions are comparable to the oscillation length at $|\Delta m^2| \sim \mathrm{eV}^2$, was assessed by assuming that antineutrinos were produced and interacted uniformly in these volumes. The impact was found to be unimportant in the range of Δm^2 where Daya Bay is most sensitive ($|\Delta m^2| < 0.3\ \mathrm{eV}^2$). Higher order effects, such as the non-uniform production of antineutrinos inside the reactor cores due to a particular reactor fuel burning history, also had a negligible impact on the final result.

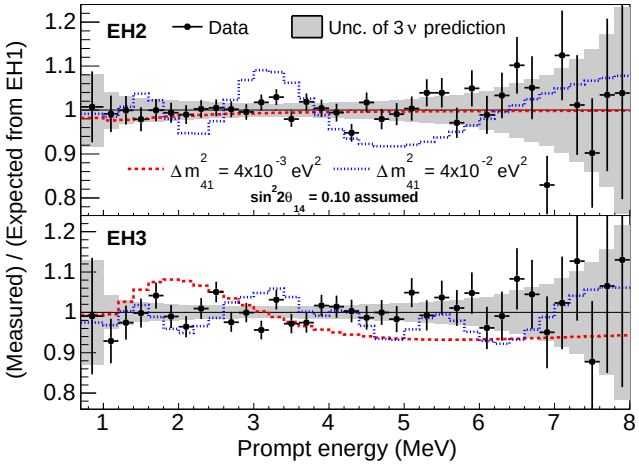

FIG. 1. (color online) Prompt energy spectra observed at EH2 (top) and EH3 (bottom), divided by the prediction from the EH1 spectrum with the three-neutrino best fit oscillation parameters from the previous Daya Bay analysis [45]. The gray band represents the uncertainty of three-neutrino oscillation prediction, which includes the statistical uncertainty of the EH1 data and all the systematic uncertainties. Predictions with $\sin^2 2\theta_{14} = 0.1$ and two representative $|\Delta m^2_{41}|$ values are also shown as the dotted and dashed curves.

The greatest sensitivity to $\sin^2 2\theta_{14}$ in the $|\Delta m^2_{41}| < 0.3\ \mathrm{eV}^2$ region came from the relative measurements between multiple EHs at different baselines. Figure 1 shows the ratios of the observed prompt energy spectra at EH2 (EH3) and the three-neutrino best fit prediction from the EH1 spectrum [45]. The data are compared with the 3+1 neutrino oscillation with $\sin^2 2\theta_{14} = 0.1$ and two representative $|\Delta m^2_{41}|$ values, illustrating that the sensitivity at $|\Delta m^2_{41}| = 4 \times 10^{-2}$ (4×10^{-3}) eV^2 came primarily from the relative spectral shape comparison between EH1 and EH2 (EH3). Sensitivities for various combinations of the data sets from differ-

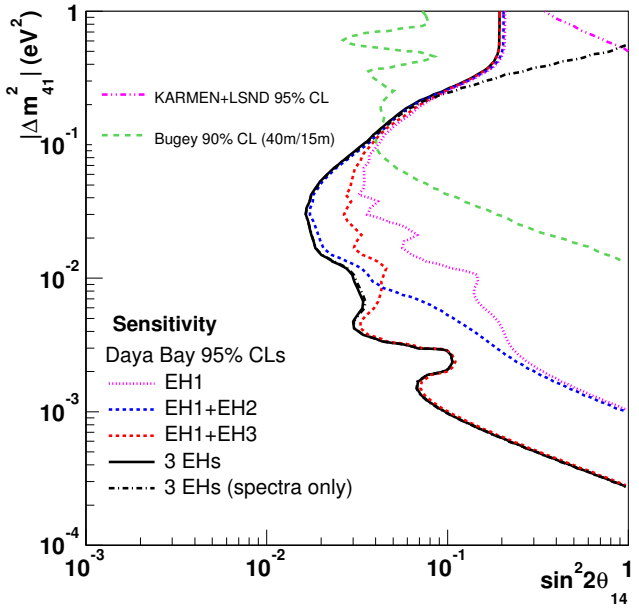

FIG. 2. (color online) Comparison of the 95% CL_s sensitivities (see text for details) for various combinations of the EH's data. The sensitivities were estimated from an Asimov Monte Carlo data set that was generated without statistical nor systematic variations. All the Daya Bay sensitivity curves were calculated assuming 5% rate uncertainty in the reactor flux except the dot-dashed one, which corresponds to a comparison of spectra only. Normal mass hierarchy was assumed for both Δm^2_{31} and Δm^2_{41}. The dip structure at $|\Delta m^2_{41}| \approx 2.4 \times 10^{-3}$ eV^2 was caused by the degeneracy between $\sin^2 2\theta_{14}$ and $\sin^2 2\theta_{13}$. The green dashed line represents Bugey's [32] 90% C.L. limit on $\overline{\nu}_e$ disappearance and the magenta double-dot-single-dashed line represents the combined KARMEN and LSND 95% C.L. limit on ν_e disappearance from ν_e-carbon cross section measurements [33].

ent EHs were estimated with the method described later in this Letter, and are shown in Fig. 2. The sensitivity in the $0.01\ \text{eV}^2 < |\Delta m^2_{41}| < 0.3\ \text{eV}^2$ region originated predominantly from the relative measurement between the two near halls, while the sensitivity in the $|\Delta m^2_{41}| < 0.01\ \text{eV}^2$ region arose primarily from the comparison between the near and far halls. The high-precision data at multiple baselines are essential for probing a wide range of values of $|\Delta m^2_{41}|$.

The uncertainty of the reactor flux model's normalization had a marginal impact in the $|\Delta m^2_{41}| < 0.3\ \text{eV}^2$ region. For $|\Delta m^2_{41}| > 0.3\ \text{eV}^2$, spectral distortion features are smeared out and the relative measurement loses its discriminatory power. The sensitivity in this region can be regained by comparing the event rates of the Daya Bay near halls with the flux model prediction, which will be reported in a future publication. In this Letter, we focus on the $|\Delta m^2_{41}| < 0.3\ \text{eV}^2$ region.

Three independent analyses were conducted, each with a different treatment of the predicted reactor antineutrino flux and systematic errors. The first analysis used the predicted reactor antineutrino spectra to simultaneously fit the data from the three halls, in a fashion similar to what was described in the recent Daya Bay spectral analysis [45]. A binned log-likelihood method was adopted with nuisance parameters constrained with the detector response and the backgrounds, and with a covariance matrix encapsulating the reactor flux uncertainties as given in the Huber [49] and Mueller [39] flux models. The rate uncertainty of the absolute reactor $\overline{\nu}_e$ flux was enlarged to 5% based on Ref. [40]. The fit used $\sin^2 2\theta_{12} = 0.857 \pm 0.024$, $\Delta m^2_{21} = (7.50 \pm 0.20) \times 10^{-5}$ eV^2 [50] and $|\Delta m^2_{32}| = (2.41 \pm 0.10) \times 10^{-3}$ eV^2 [51]. The values of $\sin^2 2\theta_{14}$, $\sin^2 2\theta_{13}$ and $|\Delta m^2_{41}|$ were unconstrained. For the 3+1 neutrino model, a global minimum of $\chi^2_{4\nu}/\text{NDF} = 158.8/153$ was obtained, while the minimum for the three-neutrino model was $\chi^2_{3\nu}/\text{NDF} = 162.6/155$. We used the $\Delta\chi^2 = \chi^2_{3\nu} - \chi^2_{4\nu}$ distribution obtained from three-neutrino Monte Carlo samples that incorporated both statistical and systematic variations to obtain a p-value [52] of 0.74 for $\Delta\chi^2 = 3.8$. The data were thus found to be consistent with the three-neutrino model, and there was no significant evidence for sterile neutrino mixing.

The second analysis performed a purely relative comparison between data at the near and far halls. The observed prompt energy spectra of the near halls were extrapolated to the far hall and compared with observation. This process was done independently for each prompt energy bin, by first unfolding it into the corresponding true antineutrino energy spectrum and then extrapolating to the far hall based on the known baselines and the reactor power profiles. A covariance matrix, generated from a large Monte Carlo dataset incorporating both statistical and systematic variations, was used to account for all uncertainties. The resulting p-value was 0.87. More details about this approach can be found in Ref. [53].

The third analysis exploited both rate and spectral information in a way that is similar to the first method but using a covariance matrix. This matrix was calculated based on standard uncertainty propagation methods, without an extensive generation of Monte Carlo samples. The obtained p-value was 0.74.

The various analyses have complementary strengths. Those that incorporated reactor antineutrino flux constraints had a slightly higher reach in sensitivity, particularly for higher values of $|\Delta m^2_{41}|$. The purely relative analysis was more robust against uncertainties in the predicted reactor antineutrino flux. The different treatments of systematic uncertainties provided a thorough cross-check of the results, which were found to be consistent for all the analyses in the region where the relative spectral measurement dominated the sensitivity ($|\Delta m^2_{41}| < 0.3\ \text{eV}^2$). As evidenced by the reported p-values, no significant signature for sterile neutrino mixing was found by any of the methods.

Two methods were adopted to set the exclusion limits in the $(|\Delta m^2_{41}|, \sin^2 2\theta_{14})$ space. The first one was a frequentist approach with a likelihood ratio as the ordering principle, as proposed by Feldman and Cousins [54]. For each point $\boldsymbol{\eta} \equiv (|\Delta m^2_{41}|, \sin^2 2\theta_{14})$, the value $\Delta\chi^2_c(\boldsymbol{\eta})$ encompassing a fraction α of the events in the $\chi^2(\boldsymbol{\eta}) - \chi^2(\boldsymbol{\eta}_{\text{best}})$ distribution was determined, where $\boldsymbol{\eta}_{\text{best}}$ was the best-fit point.

This distribution was obtained by fitting a large number of simulated experiments that included statistical and systematic variations. To reduce the number of computations, the simulated experiments were generated with a fixed value of $\sin^2 2\theta_{13} = 0.09$ [45], after it was verified that the dependency of $\Delta\chi^2_c(\boldsymbol{\eta})$ on this parameter was negligible. The point $\boldsymbol{\eta}$ was then declared to be inside the α C.L. acceptance region if $\Delta\chi^2_{\rm data}(\boldsymbol{\eta}) < \Delta\chi^2_c(\boldsymbol{\eta})$.

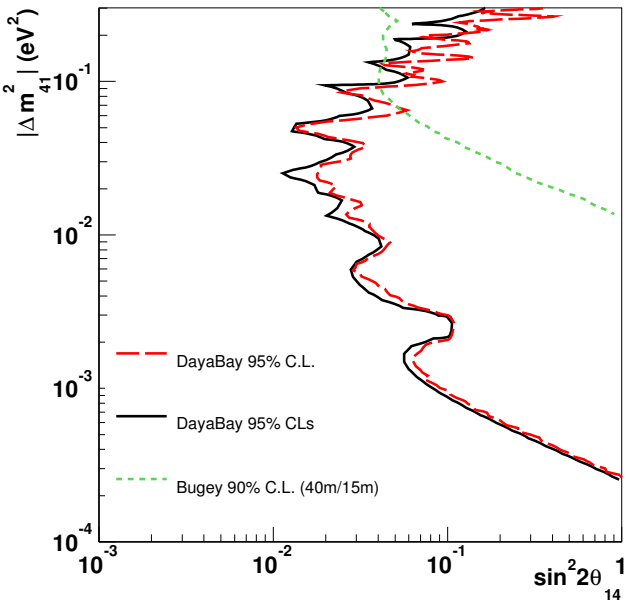

FIG. 3. (color online) The exclusion contours for the neutrino oscillation parameters $\sin^2 2\theta_{14}$ and $|\Delta m^2_{41}|$. Normal mass hierarchy is assumed for both Δm^2_{31} and Δm^2_{41}. The red long-dashed curve represents the 95% C.L. exclusion contour with Feldman-Cousins method [54]. The black solid curve represents the 95% $\rm CL_s$ exclusion contour [55]. The parameter-space to the right side of the contours are excluded. For comparison, Bugey's [32] 90% C.L. limit on $\overline{\nu}_e$ disappearance is also shown as the green dashed curve.

The second method was the $\rm CL_s$ statistical method [55] described in detail in Ref. [56]. A two-hypothesis test was performed in the ($\sin^2 2\theta_{14}$, $|\Delta m^2_{41}|$) phase space with the null hypothesis H_0 (3-ν model) and the alternative hypothesis H_1 (3+1-ν model with fixed value of $\sin^2 2\theta_{14}$ and $|\Delta m^2_{41}|$). The value of θ_{13} was fixed with the best-fit value of the data for each hypothesis. Since both hypotheses have fixed values of $\sin^2 2\theta_{14}$ and $|\Delta m^2_{41}|$, their χ^2 difference follows a Gaussian distribution. The mean and variance of these Gaussian distributions were calculated from Asimov datasets without statistical or systematic fluctuations, which avoided massive computing. The $\rm CL_s$ value is defined by:

$$\rm CL_s = \frac{1-p_1}{1-p_0}, \tag{3}$$

where p_0 and p_1 are the p-values for the 3-ν and 3+1-ν hypotheses models respectively. The condition of $\rm CL_s \leq 0.05$ was required to set the 95% $\rm CL_s$ exclusion regions.

The 95% confidence level contour from the Feldman-Cousins method and the 95% $\rm CL_s$ method exclusion contour are shown in Fig. 3. The two methods gave comparable results. The detailed structure is due to the finite statistics of the data. The impact of varying the bin size of the IBD prompt energy spectrum from 200 keV to 500 keV was negligible. Moreover, the choice of mass ordering in both the three- and four-neutrino scenarios had a marginal impact on the results. For comparison, Bugey's 90% C.L. exclusion on $\overline{\nu}_e$ disappearance obtained from their ratio of the positron energy spectra measured at 40/15 m [32] is also shown. Our result presently provides the most stringent limits on sterile neutrino mixing at $|\Delta m^2_{41}| < 0.1$ eV^2 using the electron antineutrino disappearance channel. This result is complementary to those from the $\overset{(-)}{\nu}_\mu \to \overset{(-)}{\nu}_e$ and $\overset{(-)}{\nu}_\mu \to \overset{(-)}{\nu}_\mu$ oscillation channels. While the $\overset{(-)}{\nu}_e$ appearance mode constrains the product of $|U_{\mu 4}|^2$ and $|U_{e4}|^2$, the $\overset{(-)}{\nu}_\mu$ and $\overset{(-)}{\nu}_e$ disappearance modes constrain $|U_{\mu 4}|^2$ and $|U_{e4}|^2$, respectively.

In summary, we report on a sterile neutrino search based on a minimal extension of the Standard Model, the 3 (active) + 1 (sterile) neutrino mixing model, in the Daya Bay Reactor Antineutrino Experiment using the electron-antineutrino disappearance channel. The analysis used the relative event rate and the spectral comparison of three far and three near antineutrino detectors at different baselines from six nuclear reactors. The data are in good agreement with the 3-neutrino model. The current precision is dominated by statistics. With at least three more years of additional data, the sensitivity to $\sin^2 2\theta_{14}$ is expected to improve by a factor of two for most Δm^2_{41} values. The current result already yields the world's most stringent limits on $\sin^2 2\theta_{14}$ in the $|\Delta m_{41}|^2 < 0.1$ eV^2 region.

Daya Bay is supported in part by the Ministry of Science and Technology of China, the United States Department of Energy, the Chinese Academy of Sciences, the National Natural Science Foundation of China, the Guangdong provincial government, the Shenzhen municipal government, the China Guangdong Nuclear Power Group, Key Laboratory of Particle & Radiation Imaging (Tsinghua University), Ministry of Education, Key Laboratory of Particle Physics and Particle Irradiation (Shandong University), Ministry of Education, Shanghai Laboratory for Particle Physics and Cosmology, the Research Grants Council of the Hong Kong Special Administrative Region of China, University Development Fund of The University of Hong Kong, the MOE program for Research of Excellence at National Taiwan University, National Chiao-Tung University, and NSC fund support from Taiwan, the U.S. National Science Foundation, the Alfred P. Sloan Foundation, the Ministry of Education, Youth and Sports of the Czech Republic, the Joint Institute of Nuclear Research in Dubna, Russia, the CNFC-RFBR joint research program, National Commission of Scientific and Technological Research of Chile, and Tsinghua University Initiative Scientific Research Program. We acknowledge Yellow River Engineering Consulting Co., Ltd. and China railway 15th Bureau Group Co., Ltd. for

building the underground laboratory. We are grateful for the ongoing cooperation from the China General Nuclear Power Group and China Light & Power Company.

[1] B. Pontecorvo, Sov. Phys. JETP **6**, 429 (1957).
[2] B. Pontecorvo, Sov. Phys. JETP **26**, 984 (1968).
[3] Z. Maki, M. Nakagawa, and S. Sakata, Prog. Theor. Phys. **28**, 870 (1962).
[4] J. Beringer *et al.* (Particle Data Group), Phys. Rev. D **86**, 010001 (2012).
[5] S. Schael *et al.* (ALEPH Collaboration, DELPHI Collaboration, L3 Collaboration, OPAL Collaboration, SLD Collaboration, LEP Electroweak Working Group, SLD Electroweak Group, SLD Heavy Flavour Group), Phys. Rept. **427**, 257 (2006), arXiv:hep-ex/0509008 [hep-ex].
[6] S. Dodelson and L. M. Widrow, Phys. Rev. Lett. **72**, 17 (1994), arXiv:hep-ph/9303287 [hep-ph].
[7] A. Kusenko, Phys. Rept. **481**, 1 (2009), arXiv:0906.2968 [hep-ph].
[8] M. Wyman, D. H. Rudd, R. A. Vanderveld, and W. Hu, Phys. Rev. Lett. **112**, 051302 (2014), arXiv:1307.7715 [astro-ph.CO].
[9] R. A. Battye and A. Moss, Phys. Rev. Lett. **112**, 051303 (2014), arXiv:1308.5870 [astro-ph.CO].
[10] P. Ade *et al.* (BICEP2 Collaboration), Phys. Rev. Lett. **112**, 241101 (2014), arXiv:1403.3985 [astro-ph.CO].
[11] E. Giusarma *et al.*, arXiv:1403.4852 [astro-ph.CO].
[12] J.-F. Zhang, Y.-H. Li, and X. Zhang, arXiv:1403.7028 [astro-ph.CO].
[13] M. Archidiacono, N. Fornengo, S. Gariazzo, C. Giunti, S. Hannestad, *et al.*, JCAP **1406**, 031 (2014), arXiv:1404.1794 [astro-ph.CO].
[14] B. Leistedt, H. V. Peiris, and L. Verde, arXiv:1404.5950 [astro-ph.CO].
[15] A. Aguilar *et al.* (LSND Collaboration), Phys. Rev. D **64**, 112007 (2001), arXiv:hep-ex/0104049 [hep-ex].
[16] A. Aguilar-Arevalo *et al.* (MiniBooNE Collaboration), Phys. Rev. Lett. **110**, 161801 (2013), arXiv:1303.2588 [hep-ex].
[17] A. A. Aguilar-Arevalo *et al.* (MiniBooNE Collaboration), Phys. Rev. Lett. **98**, 231801 (2007), arXiv:0704.1500 [hep-ex].
[18] M. Maltoni and T. Schwetz, Phys. Rev. D **76**, 093005 (2007), arXiv:0705.0107 [hep-ph].
[19] G. Karagiorgi, Z. Djurcic, J. Conrad, M. Shaevitz, and M. Sorel, Phys. Rev. D **80**, 073001 (2009), arXiv:0906.1997 [hep-ph].
[20] G. Karagiorgi, arXiv:1110.3735 [hep-ph].
[21] C. Giunti and M. Laveder, Phys. Lett. B **706**, 200 (2011), arXiv:1111.1069 [hep-ph].
[22] B. Armbruster *et al.* (KARMEN Collaboration), Phys. Rev. D **65**, 112001 (2002), arXiv:hep-ex/0203021 [hep-ex].
[23] P. Astier *et al.* (NOMAD Collaboration), Phys. Lett. B **570**, 19 (2003), arXiv:hep-ex/0306037 [hep-ex].
[24] N. Agafonova *et al.* (OPERA Collaboration), JHEP **1307**, 004 (2013), arXiv:1303.3953 [hep-ex].
[25] M. Antonello *et al.* (ICARUS Collaboration), Eur. Phys. J. **C73**, 2599 (2013), arXiv:1307.4699 [hep-ex].
[26] I. Stockdale *et al.*, Phys. Rev. Lett. **52**, 1384 (1984).
[27] F. Dydak *et al.*, Phys. Lett. B **134**, 281 (1984).
[28] G. Cheng *et al.* (SciBooNE and MiniBooNE Collaborations), Phys. Rev. D **86**, 052009 (2012), arXiv:1208.0322 [hep-ex].
[29] K. B. M. Mahn *et al.* (SciBooNE and MiniBooNE Collaborations), Phys. Rev. D **85**, 032007 (2012), arXiv:1106.5685 [hep-ex].
[30] S. Fukuda *et al.* (Super-Kamiokande Collaboration), Phys. Rev. Lett. **85**, 3999 (2000), arXiv:hep-ex/0009001 [hep-ex].
[31] P. Adamson *et al.* (MINOS Collaboration), Phys. Rev. Lett. **107**, 011802 (2011), arXiv:1104.3922 [hep-ex].
[32] Y. Declais *et al.*, Nucl. Phys. B **434**, 503 (1995).
[33] J. Conrad and M. Shaevitz, Phys. Rev. D **85**, 013017 (2012), arXiv:1106.5552 [hep-ex].
[34] A. Palazzo, JHEP **1310**, 172 (2013), arXiv:1308.5880 [hep-ph].
[35] A. Esmaili, E. Kemp, O. Peres, and Z. Tabrizi, Phys. Rev. D **88**, 073012 (2013), arXiv:1308.6218 [hep-ph].
[36] I. Girardi, D. Meloni, T. Ohlsson, H. Zhang, and S. Zhou, arXiv:1405.6540 [hep-ph].
[37] G. Mention *et al.*, Phys. Rev. D **83**, 073006 (2011), arXiv:1101.2755 [hep-ex].
[38] C. Zhang, X. Qian, and P. Vogel, Phys. Rev. D **87**, 073018 (2013), arXiv:1303.0900 [nucl-ex].
[39] T. Mueller *et al.*, Phys. Rev. C **83**, 054615 (2011), arXiv:1101.2663 [hep-ex].
[40] A. Hayes, J. Friar, G. Garvey, G. Jungman, and G. Jonkmans, Phys. Rev. Lett. **112**, 202501 (2014), arXiv:1309.4146 [nucl-th].
[41] W. Hampel *et al.* (GALLEX Collaboration), Phys. Lett. **B420**, 114 (1998).
[42] J. Abdurashitov *et al.* (SAGE Collaboration), Phys. Rev. C **80**, 015807 (2009), arXiv:0901.2200 [nucl-ex].
[43] C. Giunti and M. Laveder, Phys. Rev. C **83**, 065504 (2011), arXiv:1006.3244 [hep-ph].
[44] C. Giunti *et al.*, Phys. Rev. D **86**, 113014 (2012), arXiv:1210.5715 [hep-ph].
[45] F. An *et al.* (Daya Bay Collaboration), Phys. Rev. Lett. **112**, 061801 (2014), arXiv:1310.6732 [hep-ex].
[46] F. An *et al.* (Daya Bay Collaboration), Nucl. Instrum. Meth. A **685**, 78 (2012), arXiv:1202.6181 [physics.ins-det].
[47] F. An *et al.* (Daya Bay Collaboration), Chin. Phys. C **37**, 011001 (2013), arXiv:1210.6327 [hep-ex].
[48] F. An *et al.* (Daya Bay Collaboration), Phys. Rev. Lett. **108**, 171803 (2012), arXiv:1203.1669 [hep-ex].
[49] P. Huber, Phys. Rev. C **84**, 024617 (2011), arXiv:1106.0687 [hep-ph].
[50] A. Gando *et al.* (KamLAND Collaboration), Phys. Rev. D **83**, 052002 (2011), arXiv:1009.4771 [hep-ex].
[51] This value was reported in Ref. [57]. An independent measurement was recently released in Ref. [58]. Both values are consistent, and the results presented here are not very sensitive to this parameter.
[52] The p-value is the probability of obtaining a test statistic result at least as extreme as the observed one.
[53] Y. Nakajima and J. P. Ochoa-Ricoux, In preparation.
[54] G. J. Feldman and R. D. Cousins, Phys. Rev. D **57**, 3873 (1998), arXiv:physics/9711021.
[55] A. L. Read, J. Phys. G **28**, 2693 (2002).
[56] X. Qian *et al.*, arXiv:1407.5052 [hep-ex].
[57] P. Adamson *et al.* (MINOS Collaboration), Phys. Rev. Lett. **110**, 251801 (2013), arXiv:1304.6335 [hep-ex].
[58] K. Abe *et al.* (T2K Collaboration), Phys. Rev. Lett. **112**, 181801 (2014).

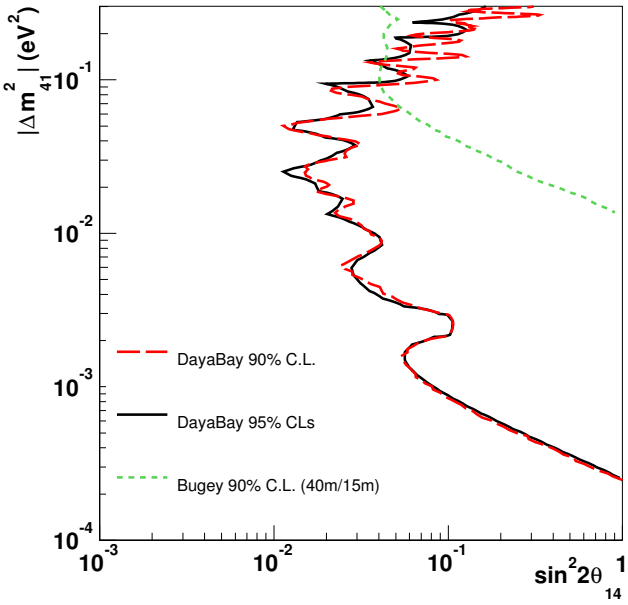

FIG. 4. Same as Fig. 3 except that the 90% C.L. exclusion contour is shown for the Feldman-Cousins method (supplemental material).